



3D Printing of Shape Memory Hydrogels with Tunable Mechanical Properties

Journal:	<i>Soft Matter</i>
Manuscript ID	SM-ART-06-2018-001156.R1
Article Type:	Paper
Date Submitted by the Author:	10-Jul-2018
Complete List of Authors:	SHIBLEE, MD NAHIN ISLAM; Yamagata University Faculty of Engineering Graduate School of Science and Engineering, Mechanical Systems Engineering Ahmed, Kumkum; Yamagata University Faculty of Engineering Graduate School of Science and Engineering, Mechanical Systems Engineering Khosla, Ajit; Yamagata University Faculty of Engineering Graduate School of Science and Engineering, Mechanical Systems Engineering Kawakami, Masaru; Yamagata University Faculty of Engineering Graduate School of Science and Engineering, Mechanical Systems Engineering Furukawa, Hidemitsu; Yamagata University, Department of Mechanical Systems Engineering



Journal Name

ARTICLE

3D printing of Shape Memory Hydrogels with Tunable Mechanical Properties

Received 00th January 20xx,
Accepted 00th January 20xx

DOI: 10.1039/x0xx00000x

www.rsc.org/

MD Nahin Islam Shiblee^a, Kumkum Ahmed^a, Ajit Khosla^a, Masaru Kawakami^{a, b} and Hidemitsu Furukawa^{a, b*}

Utilization of soft material like hydrogels for task-specific application such as soft robotics requires freedom in manufacturing process and designability. Here, we have developed highly robust thermoresponsive poly (dimethyl acrylamide-co-stearyl acrylate and/or lauryl acrylate) (PDMAAm-co-SA and/or LA)-based shape memory gels (SMGs) using a customized optical 3D gel printer. This process enabled rapid and moldless fabrication of SMGs with a variety of shapes and sizes. By varying the compositions of the constituent monomers, a wide variety of SMGs with tunable mechanical, thermal, optical and swelling properties has been obtained. Printed SMGs with excellent fixity and recovery ratio have exhibited a wide range of Young's modulus 0.04 MPa-17.35MPa and strain 612%-2363% at room temperature when acrylate co-monomer (SA and LA) content was varied and the value of strain has been found to enhance at elevated temperature. Thermogravimetric analysis (TGA) of the SMGs shows one step peak degradation (407°C- 417°C) regardless of compositions after initial mass loss for water evaporation. Dynamic mechanical analysis (DMA) and Differential scanning calorimetry (DSC) revealed variable transition temperatures (29°C-49.5°C) depending on the SA and LA content. SMGs at all the compositions possess high transparency with variable swelling degrees in water and different organic solvents and exhibits refractive index value in the range of intraocular lens making them suitable for application in the optical field. These unique properties of 3D printed SMGs with free formability and tunable properties are expected to generate rapid demand in a variety of sectors in biomedicine, robotics and sensing application.

Introduction

Over the last decade, additive manufacturing (AM) or more widely known as 3D printing has accentuated among various research fields such as, physical models,¹ tissue engineering,² electronics devices,³ microfluidics,⁴ MEMS, automotive and high specific strength materials.⁵ To foster this technology to the next level, development of wide variety of functional materials is imperative. As currently feasible functional materials for 3D printing are limited, hence there is a drive to develop 3D printable smart or intelligent materials like shape memory polymers, hydrogels and alloys which will create new scope in the emerging field of material engineering.⁶ Stimuli-sensitive smart polymers thus gained remarkable popularity in printing technology as these materials have the unique competency to return from a temporary deformed state to their permanent i.e. original shape induced by heat, light, ultrasound, chemical substances etc.⁷⁻¹¹ These materials have

been reported to be advantageous in applications including intelligent devices, such as sensors and actuators,¹² artificial insulin-control systems,¹³ efficient bio-separation devices and other bio-based technologies.¹⁴⁻¹⁷ Designability of these materials with 3D printer not only enhance visual effects but also include further benefits towards their engineering application. Owing to the geometric freedom, cost effectiveness and easy and rapid fabrication of complex design, this technology is playing important function to eliminate limitations associated with design and cost during traditional mold processing. Thus, 3D printing can be regarded as one of the indispensable part of material engineering where stimuli responsible materials being in the spotlight. A variety of shape deformable polymers and gels have been fabricated by 3D printing with the targeting applications such as actuator valve, biomimetic actuation, self-foldable and healable materials for engineering and biomedical purposes.¹⁸⁻²³ However, a very limited number of materials and methods are currently viable for this technology especially in fabrication of shape morphing hydrogels. Therefore, aiming at adding new materials in the 3D printing area, here we have fabricated a series of poly (dimethyl acrylamide-co-stearyl acrylate and/or lauryl acrylate) (PDMAAm-co-SA and/or LA) based shape memory hydrogels named as SMG via simple optical printing method commonly known as stereolithographic process and investigated their physical properties which has been tuned

^a Department of Mechanical Systems Engineering, Graduate School of Science and Engineering, Yamagata University, Jonan 4-3-16, Yonezawa, Yamagata 992-8510, Japan Address here.

^b Life-3D Printing Innovation Center, Yamagata University, 4-3-16 Jonan, Yonezawa City, Yamagata, 992-8510 Japan

Electronic Supplementary Information (ESI) available: [details of any supplementary information available should be included here]. See DOI: 10.1039/x0xx00000x

just by adjusting the concentration of monomeric constituents according to the desired requirements. The SMG in this work is composed of a hydrophilic monomer N, N- dimethyl acrylamide (DMAAm) and hydrophobic crystalline monomer SA and LA that are responsible for showing shape memory activity.

The main challenges to prepare the SMG samples via mold technique is choosing appropriate substrate or container for synthesis as DMAAm is highly adhesive to glass, metal etc. Moreover, making desired shape for any target application is very time consuming and expensive without 3D printing. Even though the first report on a similar kind of white shape transformable gels were reported by Osada *et al.* in 1995,⁷ however, till to date no major implementation has been occurred. Later our research group has developed tough and transparent SMG and made some approaches to apply the SMGs in various possible applications where shaping them to desired manner has been the major issue.²³⁻²⁸ Unlike polymers and composites, hydrogels undergo volume transformation after swelling in water which makes their fabrication via mold technique more complex and time consuming as after swelling, hydrogels change their size. To achieve actual size of hydrogels via mold technique we must repeat all the steps including rescaling the mold, manufacturing of mold and then finally dealing with the polymerizing process of gel solutions. On the other hand, 3D printing makes it easy to repeat the process effortlessly as in this case the only task is to modify the CAD file as per requirement. So, fabrication of soft materials such as hydrogels-based systems, 3D printing will be more convenient way of fabrication than mold techniques. Eventually, to find the solution of the existent problems in this work, for the first time as far as we know, we have demonstrated 3D printability of SMGs and presented a

systematic study of 3D printable SMGs and extensively studied mechanical, thermal, optical and swelling properties. Influence of chain length variation of hydrophobic content in gel matrix on the physical properties has also been studied. The conditions and properties of 3D printed SMG will trigger finding appropriate application in various fields, such as 4D printing, actuation, and sensing in soft robotics.

Experimental

Materials

Hydrophilic monomer DMAAm was purchased from Tokyo Chemical Industry Co. Ltd. Crystalline hydrophobic monomer SA and LA, crosslinker N-N' methylenbisacrylamide (MBAA), Initiator α -ketoglutaric acid (α -keto) were purchased from Wako Pure Chemical Industries, Ltd. UV absorber 5-benzoyl-4-hydroxy-2- methoxybenzenesulfonic acid (Kemisorp 11S) was purchased from Sigma-Aldrich Co., Ltd. The chemical structures of the monomers, crosslinker, initiator and UV - absorber are shown in Figure 1. Organic solvents n-hexane, diethyl ether, cyclohexane, tetrahydrofuran (THF), dichloromethane (DCM), ethanol, acetone, chloroform, tetrahydrofuran (THF), Acetic anhydrate, dimethyl sulfoxide (DMSO) are obtained either from Wako Pure chemical or from Sigma- Aldrich.

3D Printing of SMG

Solution Preparation: Gel solutions for printing has been prepared by mixing monomers, crosslinker, initiator and UV absorber respectively to a particular ratio. Composition of the components are listed in Table 1 and gels are termed as SMG75-SA20-LA05, SMG75-SA05-LA20, SMG75-SA12.5-LA12.5, SMG75-SA25-LA0 and SMG80-SA15-LA05. Gel solutions have been stirred for 15 minutes at 60 °C with continuous supply of N₂ gas to create inert environment. Five different compositions have been prepared depending on the DMAAm, SA and LA content.

Table 1: Chemical composition of SMGs during 3D printing varying hydrophilic and hydrophobic component in polymer matrix

Gel Samples	DMAAm (M)	SA (M)	LA (M)	MBAA (mol%)	α -Keto (mol%)	Kemisorp 11s (wt%)
SMG75-SA20-LA05	0.75	0.20	0.05	0.05	0.60	0.05
SMG75-SA05-LA20	0.75	0.05	0.20	0.05	0.60	0.05
SMG75-SA12.5-LA12.5	0.75	0.125	0.125	0.05	0.60	0.05
SMG75-SA25-LA0	0.75	0.25	0.0	0.05	0.60	0.05
SMG80-SA15-LA05	0.80	0.15	0.05	0.05	0.60	0.05

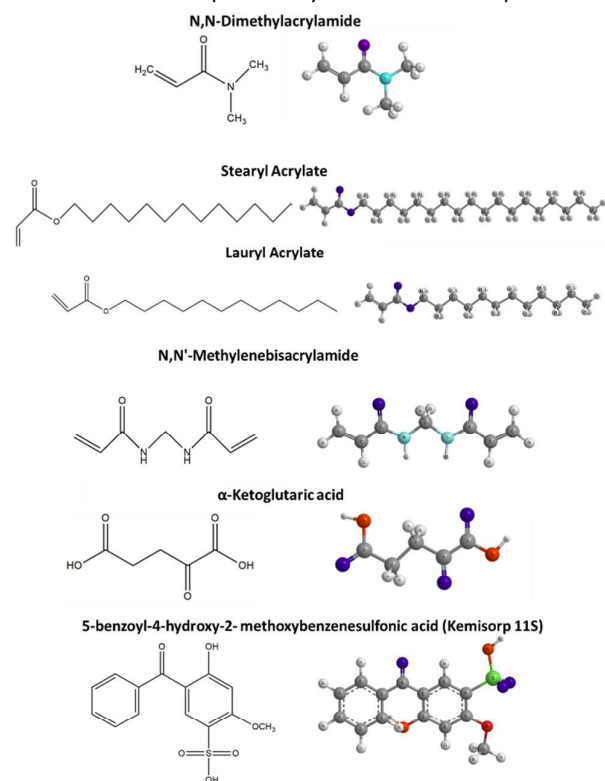


Figure 1. Chemical structure of monomer, crosslinker, initiator and UV-absorber of SMG

3D Printing: The customized 3D printer named "Soft and Wet Intelligent Matter-Easy Realizer" (SWIM-ER) has been utilized to fabricate SMG sample via optical method of stereolithography. The pre-gel solutions have been poured into a bathtub and the height of the laser source has been adjusted so that the distance between the irradiation head and the solution layer of the bathtub is equal to the focal length of the laser (laser spot diameter 0.36mm). In a first approach, easy shapes like square shaped gel sheets of

100×100 mm have been designed using a CAD software along with their path trajectories and converted for 3D printing by a printer software. The light irradiated from the irradiation head was set at 80 mW with scanning speed of 12 mm/s and 0.5mm pitch between each line. The number of scans has been optimized to complete polymerization of gel network. Number of scan and speed are important parameters to get SMGs with required mechanical properties and transparency. For printing of gel models of different shapes bathtub process according to

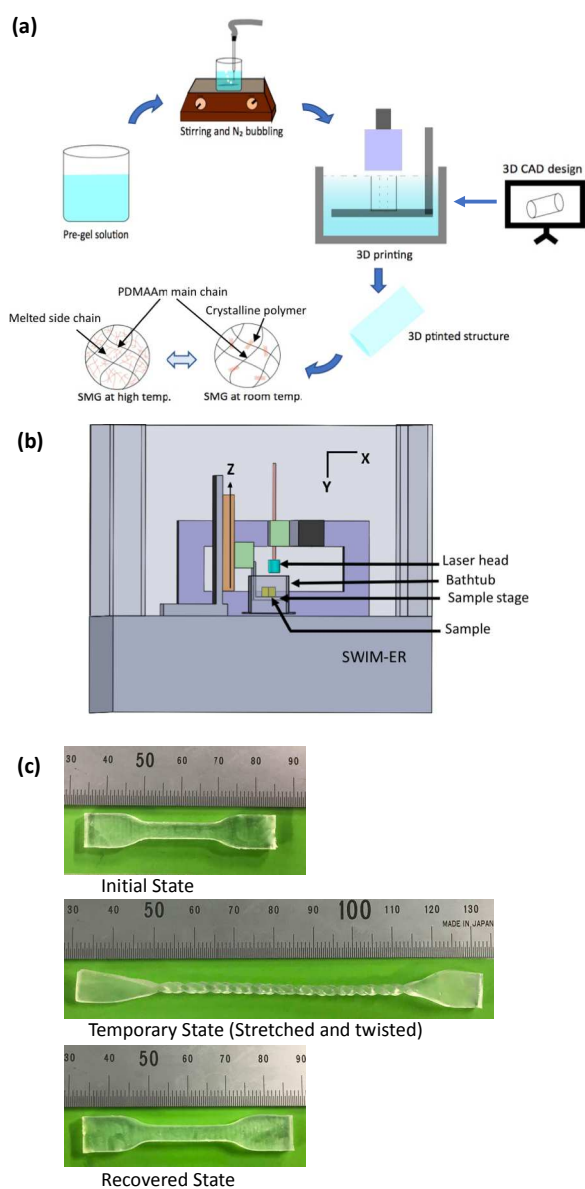


Figure 2. (a) Schematic fabrication process of SMG by 3D printing and demonstration of their internal structure modification under applied heat (b) Schematic image of 3D printer showing different parts and (c) Demonstration of shape memory effect of 3D printed dumbbell shaped SMG (PDMAAm-co-SA)

Figure 1 has been applied where the z axis pitch has been set to 0.5mm and the speed has been selected according to the design. All the printing has been performed at room temperature. The printed models are demonstrated in Figure 3 where various types of structures from simple sheet to complex architecture like finger have been possible. It can be noted here that only a certain composition of monomer and initiator result in a successful printing. Initiator and UV absorber have been optimized through successive way until the perfect combination has been achieved. After printing the gel models, they were treated in UV chamber followed by washing in alcohol solutions to remove unreacted monomers in the gel medium and finally emerged in a large amount of water to achieve the equilibrium swollen state of SMGs in water.

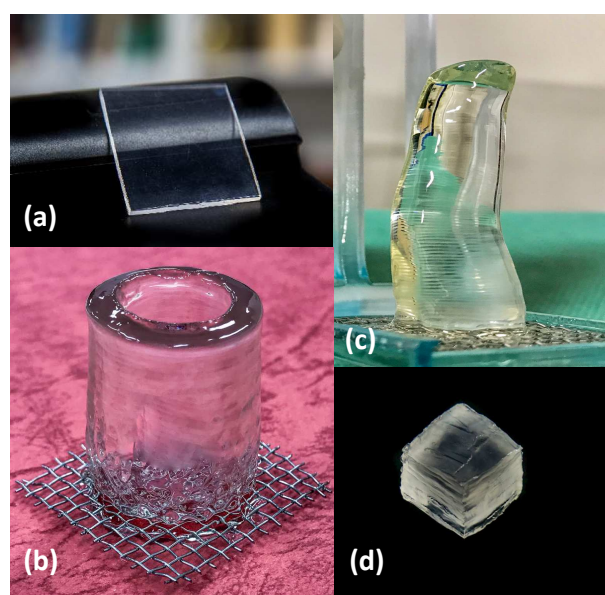


Figure 3. Images of 3D printed SMG models (a) sheet (30mm×30mm) (b) hollow cylinder (height 30mm, outer diameter 20mm and inner diameter 15mm) (c) finger (height 50mm and base diameter 15mm) and (d) cube (20mm × 20mm)

Method of Characterization

Shape memory properties were characterized using a Seiko Exstar 6000 (DMS 6100) dynamic mechanical analyzer by programmed thermomechanical procedure. Samples with dimension of 6 mm (length) × 5 mm (width) × 1 mm (thickness) were first equilibrated at 70 °C for 10 min. In step 1, at a constant temperature, the sample was experienced a tensile loading till 120 mN at a rate of 15 mN/min. In step 2, at a constant loading, the sample was cooled down to -20 °C. In step 3, at a constant temperature, stress was released. Finally, in step 4, under 0 load condition the samples were reheated to 70°C to observe the recovery. The heating and cooling rate at each cycle was 2 °C/min. Tensile measurements were carried out with the ORIENTEC testing machine (model STA-1150). A

dumbbell specimen (K6251-8) shaped samples were printed with a height of 50 mm long, 4 mm wide and 1.0-2.0 mm thick. The crosshead speed during tensile test has been set to 100 mm/min. All the tensile measurements were performed in air at room temperature or in a temperature controller. Thermal stability of the composites was measured with a thermogravimetric analyzer (TGA). The mass loss for the PIL composites were evaluated using open Al pans on a Seiko Instruments thermogravimetry/differential thermal analyzer Seiko Exstar 6000 (TG-DTA 6300) from room temperature to 550 °C under nitrogen atmosphere. A heating rate of 10 °C/min has been applied and N₂ has been purged throughout the measurement with a flow rate of 200 mL/min. Differential scanning calorimetry (DSC) has been performed using Seiko EXSTAR 6200 DSC analyser under a continuous N₂ gas flow with a flow rate of 100 mL/min. DSC thermogram was recorded in the range of -40 to 130 °C with a heating rate of 10°C/min. DMA was performed on SMG sheets (20 mm in length, 5mm in width and 0.5mm in thickness) under N₂ environment using a Seiko Exstar 6000 (DMS 6100) dynamic mechanical analyzer in tensile mode at a frequency of 10 Hz with a heating rate of 2°C/min. The refractive index was measured using a commercially available refractometer Kyoto Electronics RA-600. The water-swollen SMG samples were cut to 5 mm in diameter and measured with the RA-600 at 30°C.

Results and Discussion

Shape Memory Properties

One set of qualitative images of shape memory properties of dumbbell shaped SMGs has been provided in figure 2(c) where SMG has been stretched and twisted at high temperature (<60 °C) in water followed by cooling down to room temperature to fix temporary deformed shape. Then the temporary shape has been recovered to its original shape by placing the SMG in hot water (Figure 2 (c)). To evaluate the shape memory properties quantitatively, cyclic thermomechanical analysis has been carried out in controlled stress mode by DMA instrument. Figure 4 demonstrates three dimensional diagrams of stress-controlled programming cycles of SMG75-SA25-LA0 and SMG75-SA20-LA05. Each sample was first equilibrated at 65 °C followed by elongated up to 120mN load at a rate of 15 mN/min (step 1). Then, at fixed load condition, the sample was cooled down to -20 °C at a rate of 2 °C/min and at this condition maximum strain (ϵ_m) was recorded (step2). At a fixed temperature, load was released at a rate of 15 mN/min (step3) and temporary strain (ϵ_t) was recorded. In the final step, stress was released followed by reheating the sample to 70 °C at a rate of 2 °C/min (step 4) to record the recovery strain (ϵ_r). The whole process (step 1-step 4) has been repeated for 3 times. Shape fixity ratio (R_f) and recovery ratio (R_r) has been calculated for each cycle by the following equation^{29,30} and summarized in table 2.

$$R_f(N) = [\epsilon_t(N)/\epsilon_m] \times 100\%$$

$R_r(N) = [\epsilon_m - \epsilon_r(N)/\epsilon_m - \epsilon_r(N-1)] \times 100\%$, where N denotes the N th cycle.

During the stress-controlled elongation, SMG samples deformed almost linearly up to the maximum strain. Fixity ratio for both the

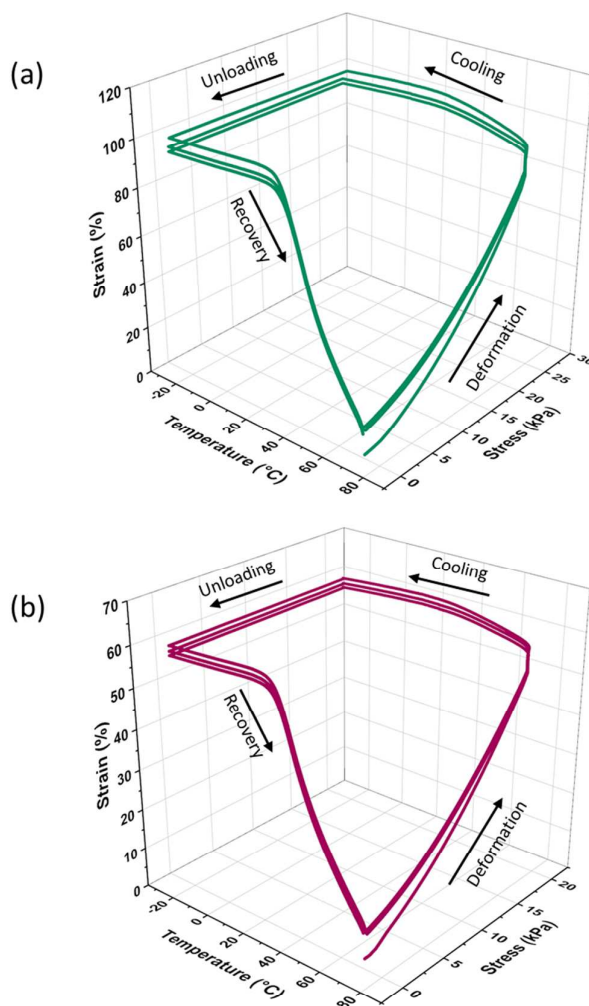


Figure 4. Shape memory properties of (a) SMG75-SA25-LA0 and (b) SMG75-SA20-LA05 characterized by stress controlled thermomechanical cycling

SMGs for each cycle displayed high fixity properties above 99% upon unloading. Upon reheating, both SMGs has shown incomplete recovery ratio around 85-87% for first cycles possibly due to the training phenomenon,²⁹ while for the following cycles excellent recovery ratio above 99% was observed (Table 2).

Mechanical Properties

Table 2: Shape memory properties of SMGs

Gel samples	Fixity ratio, R_f (%)			Recovery Ratio, R_r (%)		
	Cycle 1	Cycle 2	Cycle 3	Cycle 1	Cycle 2	Cycle 3
SMG75-SA25-LA0	99.8	99.8	99.8	87.6	99.8	99.8
SMG75-SA20-LA05	99.8	99.8	99.8	85.5	99.8	99.5

Superior mechanical properties are prerequisite for gel materials to be applied in practical applications. By controlling the amount of hydrophobic monomer LA and SA in the copolymer systems it is possible to achieve polymers with variable mechanical stiffness as LA contributes to the flexibility and SA provides rigidity in the crosslinked network. We observed that printed SMGs with high LA content is very soft (however elastic) and adhesive whereas high SA content resulted in a hard and less flexible gel materials. Tensile tests revealed composition dependent stress-strain behaviour of the SMGs and representative graph is plotted in Figure 5(b). From the Young modulus (Y.M.) values, the increasing order is SMG75-SA05-LA20 < SMG75-SA12.5-LA12.5 < SMG80-SA15-LA05 < SMG75-SA20-LA05 < SMG75-SA25-LA0 which can be well coordinated with the SA: LA ratio i.e. the Y. M. increases as the SA content increases (Table 3). Fracture point also follows the similar trend. The maximum strain has been observed for SMGs with the highest LA content (SMG75-SA05-LA20) and the enhanced flexibility reflects in the stress-strain profile of both SMG75-SA05-LA20 and SMG75-SA12.5-LA12.5, which are most stretchable SMGs. This phenomenon is possibly explained in terms of crystalline behaviour of SMGs. The monomer LA is amorphous in nature whereas the monomer SA is crystalline.³¹⁻³² As a result, in the copolymeric SMGs, the higher the SA content the greater the crystallinity and subsequently making the SMGs harder and mechanically stronger than the samples with high content of amorphous LA. It seems that by introducing the shorter chain-amorphous domain LA, the flexibility of the SMGs is easily tuned in a straightforward fashion. For realizing the sharp shape memory transition, the SA and/or LA content should be critically

to mention here that the transparency of the gels is also dependent on the proper composition of the monomer constituents. A high SA content compared to DMAAm results in turbid (white) gels due to microphase separation. It implies that that depending on the target application it is possible to fabricate the desired gels with required properties.

To estimate the mechanical properties of the SMGs at elevated temperature (30, 40, 45, 50 and 60°C) we have performed tensile tests of SMGs in a confined chamber modulating the temperature from room temperature to 60°C. As temperature increased a sharp change in the Young's Modulus (YM decreased) and stain % (strain % increased) value has been observed indicating transformation of crystalline state induced by SA to the melting state. At room temperature i.e. below the transition temperature of long chain acrylate side chains form crystalline aggregates that resembles hard plastic, while above this temperature they convert to the amorphous state through melting and the material drastically transforms to soft and flexible state that can be readily reformed to a desired temporary shape like demonstrated in Figure 2(c). The representative stress-strain curve at different temperature for tensile tests is plotted on Figure 5(b) and related quantitative data are shown in Table 4. As temperature was further increased to 50 and 60 °C the flexibility of the gels has been further increased and the gels were so soft and ductile that determination of their fracture point was not possible due to testing machine limitations. Even after being stretched up to 1700% at 50 and 60 °C the SMG were able to return to their original state upon cooling and reheating.

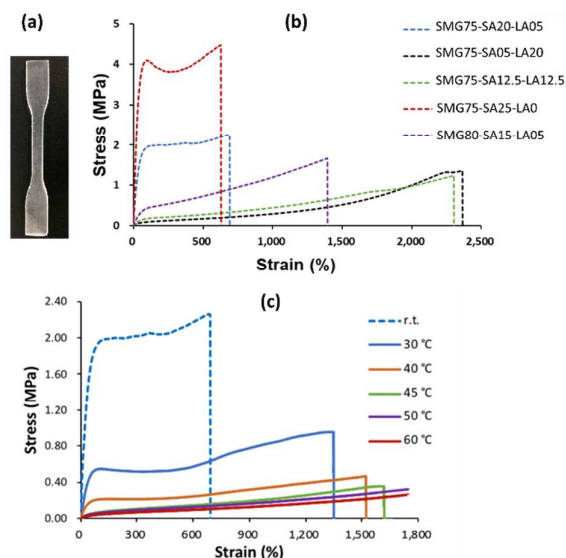


Figure 5. (a) 3D printed dumbbell shaped structure used for mechanical tests. Representative stress-strain curve for tensile tests of (b) 3D printed SMGs with different compositions at room temperature and (c) SMG75-SA20-LA05 from room temperature to 60 °C

optimized. As the content of SA is higher, the SMGs become stiffer and the reverse is true for the LA content. We would like

Table 3: Mechanical properties of SMGs at room temperature (r. t.) in swelled state

Gel Samples	SA:LA ratio in SMG	Young's Modulus (MPa)	Fracture point (MPa)	Maximum strain (%)
SMG75-SA20-LA05	4:1	7.65 ± 0.52	2.25 ± 0.15	676.09 ± 28
SMG75-SA05-LA20	1:4	0.04 ± 0.004	1.30 ± 0.078	2363.56 ± 57
SMG75-SA12.5-LA12.5	1:1	0.30 ± 0.025	1.22 ± 0.065	2283.83 ± 59
SMG75-SA25-LA0	1:0	17.35 ± 0.88	4.45 ± 0.28	612.50 ± 18
SMG80-SA15-LA05	3:1	0.89 ± 0.062	1.64 ± 0.082	1372.57 ± 37

SMG75-SA20-LA05 to SMG75-SA25-LA0 : DMAAm and hydrophobic content (SA and/or LA) ratio (3:1)
SMG80-SA15-LA05: DMAAm and hydrophobic content ratio (4:1)

Table 4: Temperature dependent mechanical properties of SMG75-SA20-LA05 in swelled state

Temperature (°C)	Youngs Modulus (MPa)	Fracture point (MPa)	Maximum strain (%)
r. t.	7.65 ± 0.52	2.25 ± 0.15	676.09 ± 28
30	1.86 ± 0.07	0.95 ± 0.08	1348 ± 36
40	0.7 ± 0.03	0.45 ± 0.03	1521 ± 45
45	0.13 ± 0.007	0.35 ± 0.02	1618 ± 51
50	0.096 ± 0.003	>0.32	>1742
60	0.08 ± 0.025	>0.26	>1742

Thermal Properties

Thermal study reveals essential information about the phase transition, degradation, stability, viscoelastic properties, damping *etc.* of materials to understand their thermo-physical properties and thus helps to find proper utilization. Thermal gravimetric analysis (TGA), Differential scanning calorimetry (DSC) and dynamic mechanical analysis (DMA) has been carried out for 3D printed SMGs to find the composition effect on the degradation temperature, transition temperature and thermomechanical properties. TGA results for SMGs show the mass reduction as a function of temperature under nitrogen purge. Approximately, 10 mg of sample was heated at a rate of 10 °C/min. According to TGA data plotted in Figure 6(a) all the SMG samples showed an initial weight loss due to the evaporation of water molecule in the SMG with mainly one-step degradation starting nearly over 360 °C with a mass loss of nearly 30wt%. TGA results of SMGs shows that thermal stability of the gels material has slight effect on the monomeric composition and the one step degradation for all the

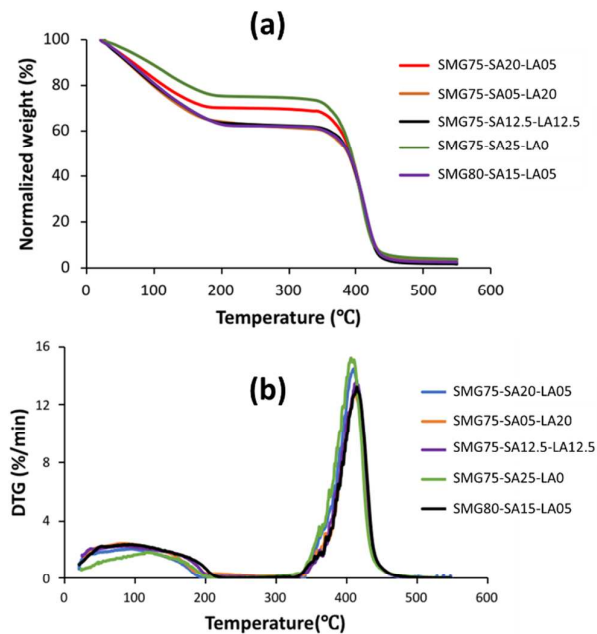


Figure 6. (a) TGA and (b) DTG of SMGs showing water evaporation and degradation of polymer network

composition proves the formation of single polymeric gels and absence on any by-product. It has been observed that SMG75-

SA25-LA0 with no LA shows obvious lower degradation peak compared to SMG with both SA and LA that proves increased crosslinking due to the shorter side chain consisting of LA. The DTG plot defines the degradation process showing a broad shoulder in the initial state for water weight loss and peak degradation has been observed at 413, 412, 415, 407 and 416 °C for SMG75-SA20-LA05, SMG75-SA05-LA20, SMG75-SA12.5-LA12.5, SMG75-SA25-LA0 and SMG80-SA15-LA05 respectively. DSC revealed information about the phase transition and crystallinity of SMGs that is significantly affected by varying composition of the hydrophobic crystalline chains as well as amorphous main chain. Endothermic melting peak near 0°C has been observed for all SMGs (Figure 7) indicating the melting of free water in the gel network. Another endothermic peak has been noticed only for SMG75-SA20-LA05, SMG75-SA25-LA0 and SMG80-SA15-LA05, due to the ordered orientation of crystalline side chains created by SA as it is already reported that homopolymer of poly-SA are more crystalline than the homopolymer of poly-LA.³³ Crystalline side chains have been formed in a well-organized fashion in SA dominant systems where the crosslinking of the SA monomer occurred within the main chain of PDMAAm and in this case LA has been found to create enhanced networking in the gel systems consequently making the structure amorphous, resembling this phenomenon in the thermogram of SMG75-SA05-LA20 and SMG75-SA12.5-LA12.5 where the melting peak disappears as the crystallinity diminishes with decreasing SA content. As it is known that with increasing the degree of crosslinking, melting enthalpy decreases and in this case the addition of LA decreases melting enthalpy along with depressing the melting temperature. SMG75-SA25-LA0 exhibited well defined melting peak at 41°C and melting peak decreases to 33°C for SMG75-SA20-LA05 and further to 29 °C for SMG80-SA15-LA05. It implies that by controlling the mole ratio of amorphous acrylamide main chain, depression of melting is altered. As above-explained in mechanical analysis, SMGs with high LA content is very soft that also implies the lack of crystallinity within the gel network. It is noted that while both SMG75-SA05-LA20 and SMG75-SA12.5-LA12.5 seem to bear no obvious crystallinity (maybe amorphous) in nature they still exhibited reversible shape changes upon heating and cooling.

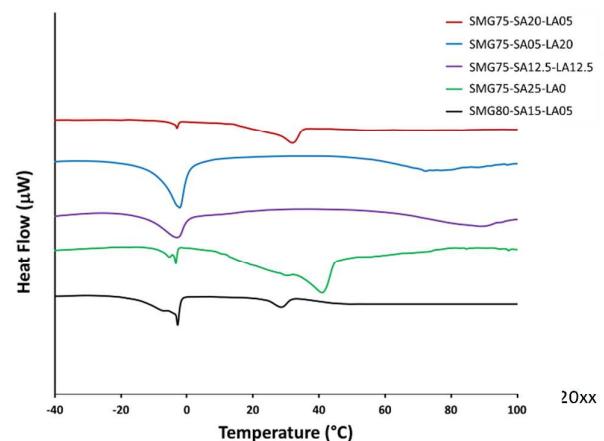


Figure 7. DSC thermogram of different SMGs with heating rate of 10 °C/min under nitrogen flow.

We have also verified the composition dependent hard to soft transition temperature by means of DMA. DMA results shown in Figure 8 (a, b) for different SMGs by varying crystalline and amorphous content exhibited storage modulus (E'), loss modulus (E'') and loss factor $\tan\delta$ (E''/E') against temperature respectively. The storage moduli for all type of SMGs have been found to be higher than the loss modulus and a gradual decrease in the modulus has been observed with increasing temperature showing transition from stiff glasslike nature to rubberlike flexible texture. SMG75-SA25-LA0 with no LA content has been observed as the stiffest among all SMGs retaining higher storage modulus until 30 °C and the onset temperature for transition in E' is observed at around 40°C. It was also observed that elastic moduli for all SMGs were of comparable value at low temperature (-60°C to 0°C) whereas at room temperature SMG with higher LA content showed

tensile test. Transition temperatures from E' , E'' and $\tan\delta$ have been put in Table 5 and the transition temperatures have been found to follow similar trend obtained from the melting peak of DSC for SMG75-SA20-LA05, SMG75-SA25-LA0 and SMG80-SA15-LA05. By DMA it was also possible to obtain information about the transition temperature of amorphous SMGs i.e. SMG75-SA05-LA20 and SMG75-SA12.5-LA12.5 which shows the lowest transition temperature. Thus, depending on the target application temperature for shape memory effect is possibly adjustable in a straightforward step by controlling the composition of amorphous and crystalline domains.

Optical Properties

One of the promising application of hydrogels in the biomedical sectors occupy in developing soft contact lenses^{34, 35} where DMAAm has been widely used in these fields. SMG exhibited RI in the range of IOL makes them suitable to be used in optical application^{26, 27}.

RI of SMGs has been found to be dependent on the polymeric SA content. In Figure 9, dependence of RI on the SA concentration has been plotted and RI has been found to increase with increasing SA concentration. SMG75-SA05-LA20 and SMG75-SA12.5-LA12.5 has exhibited the lowest RI whereas SMG75-SA25-LA0 has the highest RI in absence of LA. At room temperature, the SA domains remain in crystalline form and when light passes through the SMGs light gets reflected in this crystal domains consequently decreasing the speed of light in SMGs. As a result, RI increases proportionally with the SA content. Thus, it can be said that it is possible to achieve required RI according to the desired application. Mid-index materials like SMGs can be usable in optical apparatus by maintaining thickness and power through adjusting the monomer composition. SMG thus will be an important candidate in application of optical devices and applied to 3D printing, which will realize their optical devices more rapid and affordable, comparing to currently available technologies.

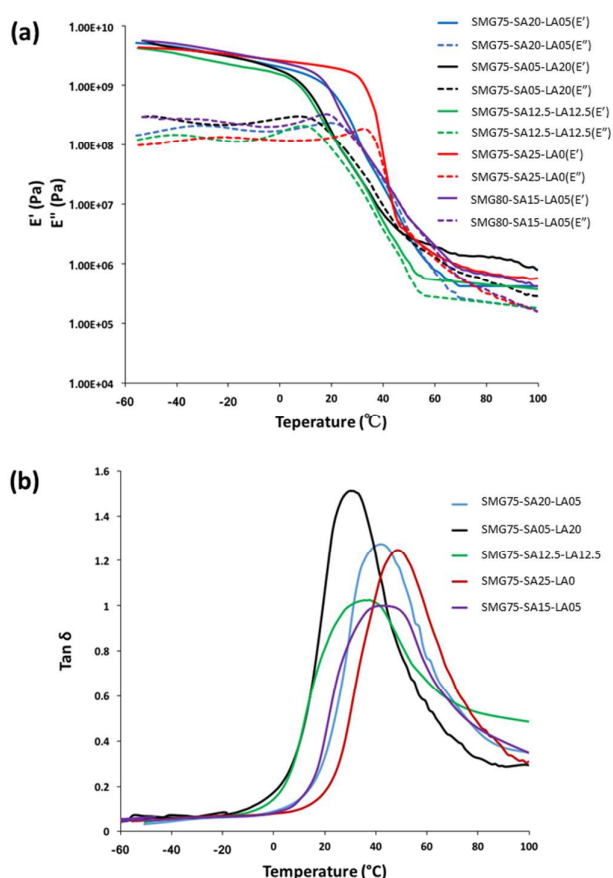


Figure 8. DMA profile of SMGs with varying composition showing a) Storage modulus (E') and Loss modulus (E'') and b) Loss factor as a function of temperature at frequency rate of 10Hz

decreased value supporting the results obtained from the

Table 5: Transition temperatures from DMA

Gel Samples	Transition Temp from E' (°C)	Transition Temp from E'' (°C)	Transition Temp from $\tan\delta$ (°C)
SMG75-SA20-LA05	20.4	22.2	41.8
SMG75-SA05-LA20	8.3	12.3	31.0
SMG75-SA12.5-LA12.5	7.3	11.0	31.8
SMG75-SA25-LA0	32.5	34.1	49.5
SMG80-SA15-LA05	15.4	18.6	44.1

Swelling Degree

Extent of swelling of gels in solvent have significant effect on the physical properties of gel. Swelling degree of SMGs in water and different solvent has been carried out and calculated by the

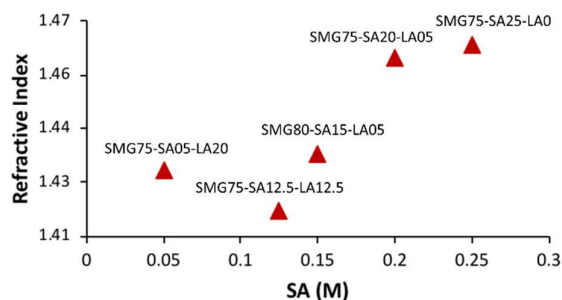


Figure 9. RI of different SMGs in swelled state as a function of SA monomer concentration

following equation.

$$\text{Swelling degree (\%)} = \frac{W_s - W_d}{W_s} \times 100,$$

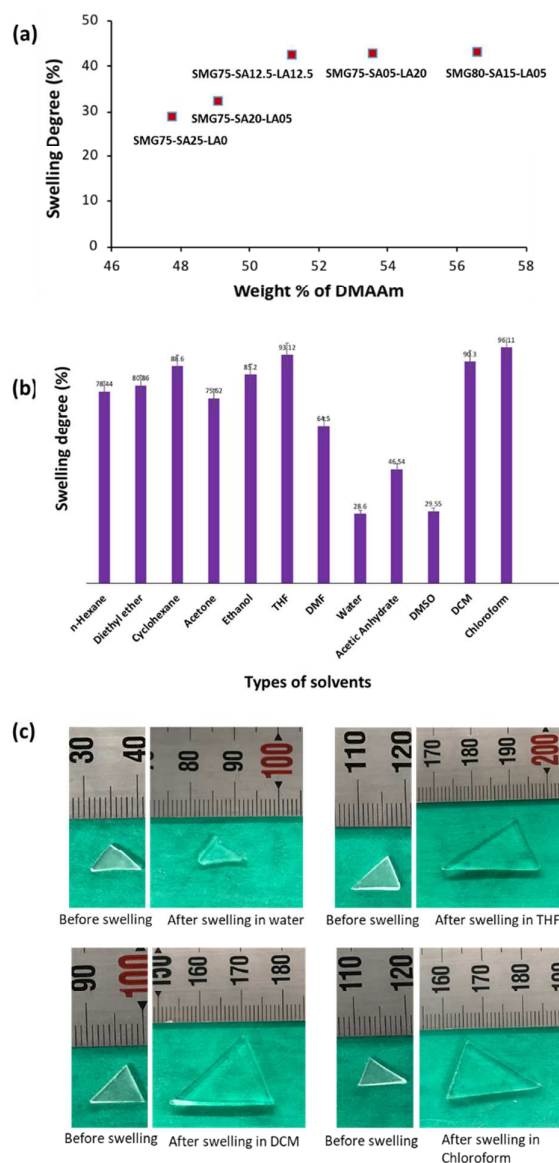


Figure 10. (a) Swelling degree of different SMGs in water as a function of wt% of DMAAm monomer (b) Swelling degree of SMG75-SA25-LA0 in various organic solvents (c) images showing shape deformation after swelling in different solvents (water, THF, DCM and chloroform)

where W_d and W_s signifies the weight of gel before and after swelling respectively. The swelling degree of the SMGs are solely governed by the hydrophilic DMAAm monomer content and this well-ordered trend has been observed that follows proportional relation with DMAAm wt% as shown in Figure 10 (a). Thus, makes it

very easy to control the hydrophilicity of the gels Swelling degree of DMAAm-co-SA (SMG75-SA25-LA0) has been also evaluated in variety of polar and non-polar solvents with increasing order of density (Figure 10 (b)). It has been found that SMG75-SA25-LA0 swell extensively in most of the organic solvents, causing that the shape memory property tends to diminish. While chloroform, DCM and THF have been found to be the most swellable solvent for SMG (swelling degree more than 90%), water has been identified as the least swellable solvent (swelling degree ~30%). It implies that the hydrophobic domains consisting of SA and LA do not get disrupted in the presence of water whereas other solvents tested plasticize these domains and therefore eliminate accessible thermal transitions. However, by removing the organic solvents from SMG shape memory property can be redeemed. Their shape changes due to swelling in water, THF, DCM and chloroform has been depicted in Figure 10 (c).

Conclusions

In summary, we successfully fabricated thermo-responsive SMGs from easy to complex shapes via 3D printing process. The characterization of these gels showed that both the hydrophilic and hydrophobic constituent have vital role in tuning their physical properties. The SMGs exhibited shape fixity ratio above 99% for all cycles and recovery ratio above 99% from the second cycle. Their mechanical properties have shown large dependence on the presence of crystalline state induced by different chain length bearing n-alkyl acrylate monomer. It was also found that enhanced toughness and flexibility has been tuned by simply altering the molar ratio of SA and LA in the hydrophilic PDMAAm matrix. Tensile tests at elevated temperature showed the sharp decrease in Young's modulus in the range of 30-50 °C and demonstrated extraordinary (a few thousand of) strain% at elevated temperature. The swelling degree of the SMGs in water has been found to have a proportional relation with the hydrophilic DMAAm wt%. Thermal properties revealed from TGA showed one step degradation of the polymeric chain after evaporation of free water and the presence of SA and/or LA in the DMAAm matrix slightly enhances the peak degradation temperature. DSC results revealed the composition dependent crystallinity of the SMG networks along with the tunability of melting temperature. DMA established the transition temperature of SMGs. Both DMA and DSC showed the same behaviour about the simple order of the transition temperature related to the composition variation. This type of 3D printed SMGs will be appropriate for various applications, for example smart optical devices in biomedical field, in manufacturing of thermo-responsive soft robots etc.

Conflicts of interest

There are no conflicts to declare.

Acknowledgements

This study was partly supported by the Grant-in-Aid for Scientific Research (Category A, Project No. 17H01224, etc.) from the Japan Society for the Promotion of Science (JSPS), the Center Of Innovation (COI) program from the Japan Science and Technology Agency (JST), the Strategic Innovation Creation Project (SIP) from the New Energy and Industrial Technology Development Organization (NEDO) of Japan, and the Program on Open Innovation Platform with Enterprises, Research Institute and Academia (OPERA) from the JST. Ahmed K. is supported by JSPS fellowship for young scientist in DC1 category. The authors acknowledge the support of Prof. Tomoya Higashihara for the access of DSC, TGA and DMA instruments.

References

- J. P. Kruth, M. C. Leu, T. Nakagawa, *CIRP Ann.* 1998, **47**, 525–540.
- H. N. Chia, B. M. Wu, *J. Biol. Eng.* 2015, **9**, 4.
- M. Zarek, M. Layani, I. Cooperstein, E. Sachyani, D. Cohn, S. Magdassi, *Adv. Mater.* 2016, **28**, 4449–4454.
- J. L. Erkal, A. Selimovic, B. C. Gross, S. Y. Lockwood, E. L. Walton, S. McNamara, R. S. Martin, D. M. Spence, *Lab Chip* 2014, **14**, 2023–2032.
- X. Zheng, H. Lee, T. H. Weisgraber, M. Shusteff, J. DeOtte, E. B. Duoss, J. D. Kuntz, M. M. Biener, Q. Ge, J. A. Jackson, S. O. Kucheyev, N. X. Fang, C. M. Spadaccini, *Science.*, 2014, **344**, 1373–1377.
- F. Momeni, S. M. Mehdi, N. Hassani, X. Liu, J. Ni, *Mater. Des.*, 2017, **122**, 42–79.
- Y. Osada, A. Matsuda, *Nature.*, 1995, **376**, 1995, 219.
- K. P. Mineart, S. S. Tallury, T. Li, B. Lee, R. J. Spontak, *Ind. Eng. Chem. Res.*, 2016, **55**, 12590.
- C. Liu, H. Qin, P. T. Mather, *J. Mater. Chem.*, 2007, **17**, 1543.
- M. Behl, A. Lendlein, *Mater. Today*, 2007, **10**, 20.
- T. Raidt, R. Hoehner, F. Katzenberg, J. C. Tiller, *Macromol. Rapid Commun.*, 2015, **36**, 744.
- B. Jeong, A. Gutowska, *Trends Biotechnol.*, 2002, **20**, 305–11.
- A. Matsumoto, R. Yoshida, K. Kataoka, *Biomacromolecules.*, 2004, **5**, 1038–45.
- W. Cai, E. C. Anderson, R. B. Gupta, *Ind. Eng. Chem. Res.*, 2001, **40**, 2283–8.
- M. Yamato, T. Okano, *Mater Today.*, 2004, **7**, 42–7.
- T. Z. Grove, C. O. Osuji, J. D. Forster, E.R. Dufresne, L. Regan, *J. Am. Chem. Soc.*, 2010, **132**, 14024–26.
- G. Pan, K. I. Kurumada, Y. Yamada, *J. Chin. Inst. Chem. Eng.*, 2008, **39** (4), 361–6.
- A. S. Wu, W. Small, T. M. Bryson, E. Cheng, T. R. Metz, S. E. Schulze, E. B. Duoss, T. S. Wilson, *Sci. Rep.* 2017, **7**, 4664.
- S. Naficy, R. Gately, R. Gorkin, H. Xin and G. M. Spinks, *Macromol. Mater. Eng.*, 2017, **302**, 1–9.
- A. S. Gladman, E. A. Matsumoto, R. G. Nuzzo, L. Mahadevan, J. A. Lewis, *Nat. Mater.*, 2016, **15**, 413–419.
- S. E. Bakarich, R. Gorkin, G. M. Spinks, *Macro. Rap. Comm.*, 2015, **36**, 1211–1217.
- L. Huang, R. Jiang, J. Wu, J. Song, H. Bai, B. Li. Q. Zhao, T. Xie, *Adv. Mater.* 2017, **29**, 1605390.
- M. H. Kabir, T. Hazama, Y. Watanabe, J. Gong, K. Murase, T. Sunada, H. Furukawa, *J. Taiwan. Inst. Chem. Eng.*, 2014, **45** (6) 3134–3138.
- H. Kumagai, K. Sakai, M. Kawakami, H. Furukawa, K. Murase, T. Sunada, *Microsyst Technol.*, 2018, **24**, 725.
- M. Wada, R. Hidema, T. Chiba, K. Yamada, N. Yamada, J. Gong and H. Furukawa, *J. Solid Mech. Mater. Eng.*, 2013, **7**, 228–234.
- S. Harada, R. Hidema, J. Gong and H. Furukawa, *Chem. Lett.*, 2012, **41**, 1047–1049.
- T. Yokoo, R. Hidema and H. Furukawa, *e-Journal Surf. Sci. Nanotechnol.*, 2012, **10**, 243–247.
- H. Muroi, R. Hidema, J. Gong and H. Furukawa, *J. Solid Mech. Mater. Eng.*, 2013, **7**, 163–168.
- I. A. Rousseau, *Polym. Eng. Sci.*, 2008, **48**, 2075–2089.
- T. Defize, R. Riva, J. M. Raquez, P. Dubois, C. Jerome, M. Alexandre, *Macromol. Rapid Commun.*, 2011, **32**, 1264–1269.
- E. F. Jordan, B. Artymyshyn, A. Specca, A. N. Wrigley, *J. Polym. Sci. A-1 Polym. Chem.*, 1971, **9**, 3349–3365
- R. J. Leyrer, W. Machtle, *Macromol. Chem. Phys.*, 2000, **201**, 1235–1243.
- F. Dutertre, P. Pennarun, O. Colombani, E. Nicol, *Eur. Polym. J.*, 2011, **47** (3), 343–351.
- N. A. Peppas, Y. Huang, M. Torres-Lugo, J.H. Ward, J. Zhang *Annu. Rev. Biomed. Eng.* 2000, **2**, 9–29.
- T. Kaneko, S. Tanaka, A. Ogura, A. Mitsuru, *Macromolecules.*, 2005, **38**, 4861–7.

Title: 3D printing of Shape Memory Hydrogels with Tunable Mechanical Properties

TOC

Highly robust and mechanically tunable 3D printable thermo-responsive hydrogels have been developed and characterized

